Heme Oxygenase-1 Regulates Myeloid Cell Trafficking in AKI

Travis D. Hull,*† Ahmed I. Kamal,* Ravindra Boddu,* Subhashini Bolisetty,* Lingling Guo,*† Cornelia C. Tisher,* Sunil Rangarajan,* Bo Chen,*‡ Lisa M. Curtis,*§ James F. George,*† and Anupam Agarwal*§

*Nephrology Research and Training Center, ‡Division of Nephrology, Department of Medicine, and †Division of Cardiothoracic Surgery, Department of Surgery, University of Alabama at Birmingham, Birmingham, Alabama; and §Birmingham Veterans Administration Medical Center, Birmingham, Alabama

ABSTRACT

Renal ischemia-reperfusion injury is mediated by a complex cascade of events, including the immune response, that occur secondary to injury to renal epithelial cells. We tested the hypothesis that heme oxygenase-1 (HO-1) expression, which is protective in ischemia-reperfusion injury, regulates trafficking of myeloid-derived immune cells in the kidney. Age-matched male wild-type (HO-$1^{+/+}$), HO-1–knockout (HO-$1^{-/-}$), and humanized HO-1–overexpressing (HBAC) mice underwent bilateral renal ischemia for 10 minutes. Ischemia-reperfusion injury resulted in significantly worse renal structure and function and increased mortality in HO-$1^{-/-}$ mice. In addition, there were more macrophages ($CD45^+$ $CD11b^{hi}F4/80^{lo}$) and neutrophils ($CD45^+$ $CD11b^{hi}$ $MHCII^-$ $Gr\text{-}1^{hi}$) in HO-$1^{-/-}$ kidneys than in sham and HO-$1^{+/+}$ control kidneys subjected to ischemia-reperfusion. However, ischemic injury resulted in a significant decrease in the intrarenal resident dendritic cell (DC; $CD45^+MHCII^+CD11b^{lo}F4/80^{hi}$) population in HO-$1^{-/-}$ kidneys compared with controls. Syngeneic transplant experiments utilizing green fluorescent protein–positive HO-$1^{+/+}$ or HO-$1^{-/-}$ donor kidneys and green fluorescent protein–negative HO-$1^{+/+}$ recipients confirmed increased migration of the resident DC population from HO-$1^{-/-}$ donor kidneys, compared to HO-$1^{+/+}$ donor kidneys, to the peripheral lymphoid organs. This effect on renal DC migration was corroborated in myeloid-specific HO-$1^{-/-}$ mice subjected to bilateral ischemia. These mice also displayed impaired renal recovery and increased fibrosis at day 7 after injury. These results highlight an important role for HO-1 in orchestrating the trafficking of myeloid cells in AKI, which may represent a key pathway for therapeutic intervention.

J Am Soc Nephrol 26: 2139–2151, 2015. doi: 10.1681/ASN.2014080770

AKI is an intractable clinical condition associated with significant morbidity and mortality.[1,2] Epithelial injury and death, circulatory dysfunction, and immunologic factors from the circulation or within the kidney influence the integrity of the renal parenchyma and determine the outcome of AKI.[3,4] The innate immune system, which includes cells of the myeloid lineage such as neutrophils, circulating monocytes, tissue macrophages, dendritic cells (DCs), and their precursors, is a key contributor to the pathogenesis and resolution of AKI.[5–7] Ischemia-reperfusion injury (IRI) is a common cause of AKI in clinical settings such as major cardiac surgery, hypovolemic shock, and renal transplantation.[8–11] The

Received August 12, 2014. Accepted October 22, 2014.

T.D.H. and A.I.K. contributed equally to this work.

Published online ahead of print. Publication date available at www.jasn.org.

Present address: Dr. Ahmed I. Kamal, Mansoura Urology and Nephrology Center, Mansoura University, Mansoura, Egypt.

Correspondence: Dr. Anupam Agarwal, Division of Nephrology, Department of Medicine, University of Alabama at Birmingham, 1720 Second Avenue South, Room 647 THT, Birmingham, AL 35294, or Dr. James F. George, Division of Cardiothoracic Surgery, Department of Surgery, University of Alabama at Birmingham, Room 780 LHRB, 1720 Second Avenue South, Birmingham, AL 35294. Email: agarwal@uab.edu or jgeorge@uab.edu

pathogenesis of IRI involves crosstalk between the kidney parenchyma and the immune system, with effects on renal hemodynamics and tubular injury.[12,13]

Heme oxygenase-1 (HO-1) is an important cytoprotective enzyme that regulates the inflammatory response to tissue injury.[14,15] Its induction is a protective response in renal IRI and other forms of AKI.[16,17] HO-1 expression decreases neutrophil infiltration after acute tissue injury.[18] In addition, HO-1 expression in DCs regulates their ability to undergo maturation and antigen presentation in lymphoid tissues.[14,19–21] Because of its emerging role in immune regulation and transplantation, we hypothesized that HO-1 expression plays a critical role in the response to renal IRI by modulating the trafficking of myeloid cells into the kidney as well as controlling emigration of renal mononuclear cells (RMNCs), defined as hematopoietically derived $CD11b^+$ $MHCII^+$ cells residing within the renal parenchyma, to the peripheral lymphoid organs. We utilized transgenic mice with systemic ($HO\text{-}1^{-/-}$) or myeloid-specific ($HO\text{-}1^{LysM-/-}$) HO-1 deficiency as well as humanized HO-1 mice that lack mouse HO-1 but overexpress the human HO-1 gene on a bacterial artificial chromosome (HBAC),[22] to study the effects of HO-1 on renal inflammation and the intrarenal RMNC population. We also used syngeneic kidney transplantation with green fluorescent protein–positive (GFP^+) $HO\text{-}1^{+/+}$ and (GFP^+) $HO\text{-}1^{-/-}$ donor kidneys into green fluorescent protein–negative (GFP^-) $HO\text{-}1^{+/+}$ recipients to evaluate the role of HO-1 in trafficking of myeloid cells after IRI.

RESULTS

HO-1 Deficiency Increases Susceptibility to Renal IRI

HO-1–deficient mice are extremely susceptible to renal IRI.[23] Therefore, we used a short ischemia time (10 minutes), which was sublethal in $HO\text{-}1^{+/+}$ mice, but resulted in 50% mortality after 1 day of reperfusion, and 60% mortality by day 2 in $HO\text{-}1^{-/-}$ mice ($P<0.05$) (Figure 1A). Serum creatinine was significantly elevated by day 1 in $HO\text{-}1^{-/-}$ mice compared with $HO\text{-}1^{+/+}$ mice ($P\leq0.01$) and sham-operated control mice (Figure 1B). In $HO\text{-}1^{-/-}$ mice that survived to day 7, serum creatinine was not significantly different from baseline levels or $HO\text{-}1^{+/+}$ controls. Overexpression of human HO-1 in HBAC mice rescued the mortality and decline in kidney function observed in $HO\text{-}1^{-/-}$ mice (Figure 1).

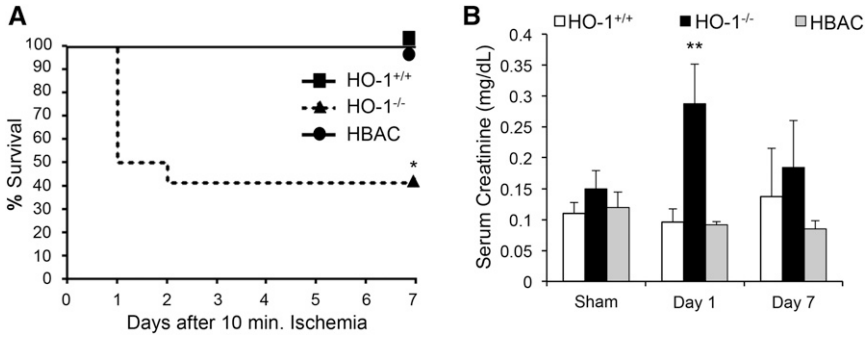

Figure 1. $HO\text{-}1^{-/-}$ mice exhibit increased susceptibility to renal IRI. (A) Kaplan–Meier survival plot demonstrating mortality over 7 days in $HO\text{-}1^{+/+}$ (n=10), $HO\text{-}1^{-/-}$ (n=12), and HBAC (n=6) mice subjected to 10 minutes of IRI. *$P<0.05$ versus $HO\text{-}1^{+/+}$ and HBAC. (B) Serum creatinine levels in sham-operated mice and after 1 or 7 days of IRI. Results are presented as the mean±SEM. **$P<0.01$ in $HO\text{-}1^{-/-}$ versus $HO\text{-}1^{+/+}$ and HBAC mice at day 1. n=6–12 for IRI groups and n=3–4 for sham groups.

HO-1 Expression Prevents Tubulointerstitial Damage and Renal Fibrosis after IRI

There appeared to be no differences in renal histology in $HO\text{-}1^{+/+}$, $HO\text{-}1^{-/-}$, and HBAC mice subjected to sham surgery. However, significant injury was evident in $HO\text{-}1^{-/-}$ kidneys at day 1 after IRI, with extensive brush border loss in the proximal tubules, cast formation, and necrotic tubules. These features were not present in $HO\text{-}1^{+/+}$ and HBAC kidneys subjected to IRI (Figure 2A). At day 7 after IRI, cast formation was increased in $HO\text{-}1^{-/-}$ mice compared with $HO\text{-}1^{+/+}$ controls. Analysis of renal fibrosis by picrosirius red staining 7 days after IRI revealed increased collagen deposition in $HO\text{-}1^{-/-}$ kidneys compared with $HO\text{-}1^{+/+}$ and HBAC kidneys (Figure 2B). Western blotting demonstrated increased expression of both α smooth muscle actin (Figure 2C) and fibronectin (Figure 2D) in $HO\text{-}1^{-/-}$ kidneys subjected to IRI.

HO-1 Deficiency Alters the Trafficking of Myeloid-Derived Immune Cells after IRI

Single cell suspensions from perfused kidneys harvested 1 day after 10 minutes of ischemia were analyzed by flow cytometry (Figure 3A). The proportion of bone marrow–derived ($CD45^+$) cells was significantly elevated in $HO\text{-}1^{-/-}$ kidneys subjected to IRI compared with kidneys from $HO\text{-}1^{+/+}$ and HBAC mice ($P\leq0.01$) (Figure 3, B and D). Further characterization of $CD45^+$ cells revealed significant neutrophil ($CD45^+$ $CD11b^{hi}$ $MHCII^-$ $Gr\text{-}1^{hi}$; Figure 3A) infiltration in $HO\text{-}1^{-/-}$ kidneys compared with $HO\text{-}1^{+/+}$ and HBAC kidneys subjected to IRI ($P\leq0.001$) and sham kidneys (Figure 3, C and E). Seven days after ischemia, there were no significant differences in neutrophil infiltration (data not shown).

IRI also resulted in a striking decrease in the proportion of $CD45^+$ $CD11b^+$ $MHCII^+$ cells (hereafter called RMNCs; Figure 3, A, C, and F) in $HO\text{-}1^{-/-}$ kidneys compared with $HO\text{-}1^{+/+}$ and HBAC mice ($P\leq0.001$). There was no significant difference in sham-operated mice, suggesting that the decrease of RMNCs in $HO\text{-}1^{-/-}$ mice is a specific response to kidney injury. The observed decrease in RMNCs between $HO\text{-}1^{-/-}$ kidneys subjected to sham and IRI ($P\leq0.001$) may be explained by trafficking of RMNCs from the injured kidney.

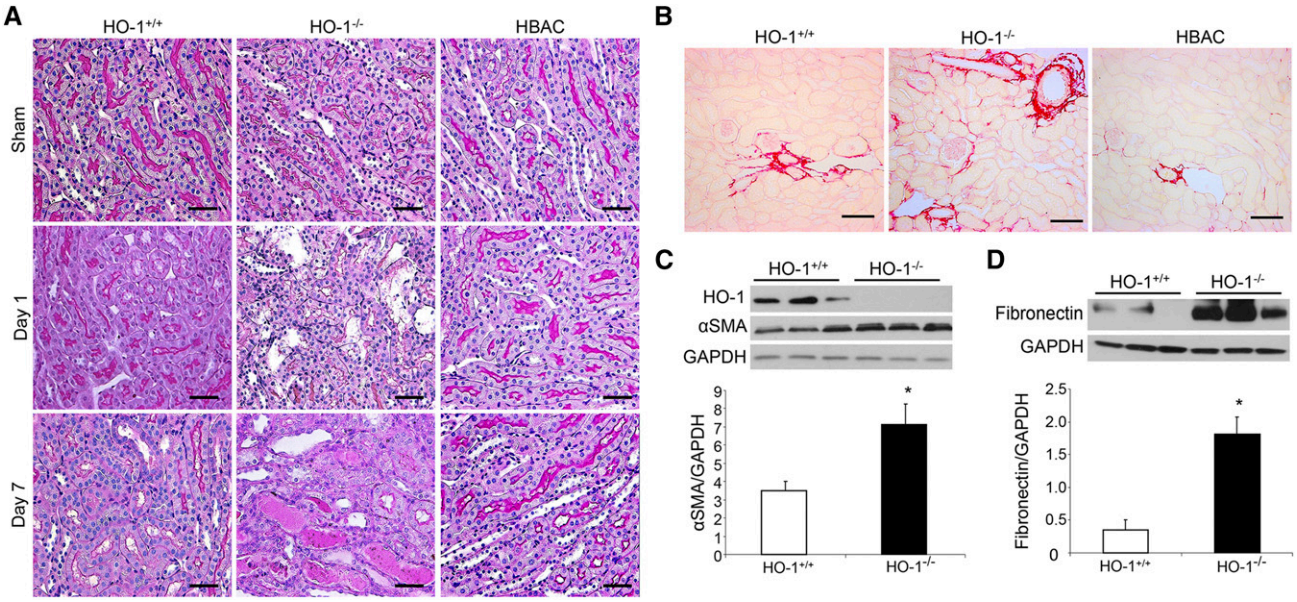

Figure 2. HO-1 expression prevents tubulointerstitial damage and renal fibrosis after IRI. (A) Representative micrographs demonstrating tubulointerstitial damage in the outer medulla of kidneys from HO-$1^{+/+}$, HO-$1^{-/-}$ or HBAC mice subjected to sham surgery or 1 or 7 days of reperfusion after 10 minutes of ischemia. Transverse sections are stained with periodic acid–Schiff. n=4 per group. (B) Picrosirius red staining of kidney sections from HO-$1^{+/+}$, HO-$1^{-/-}$, and HBAC kidneys 7 days after IRI. n=4 per group. (C and D) Western blot analysis and densitometric quantification of the fibrosis markers α-smooth muscle actin (α-SMA) (C) and fibronectin (D) at day 7 after IRI. GAPDH is used as a loading control and for normalization of densitometry values. n=3 per group. *$P \leq 0.05$. Scale bar, 200 μm in A; 100 μm in B.

The predominant population of immune cells in the quiescent kidney is F4/80^{hi} CD11b^{lo}, although a second smaller population of F4/80^{lo} CD11b^{hi} cells is also present and significantly increases after IRI.[24] These cells have been previously defined as DCs and macrophages, respectively, and will be referred to as such hereafter.[24,25] We confirmed this previously reported finding by analyzing RMNC expression of F4/80 in the quiescent kidney and after IRI (Figure 4, Supplemental Figure 1). As expected, the F4/80^{hi} CD11b^{lo} population (DCs) predominates in the kidneys of mice subjected to sham surgery, with no significant difference between macrophages or DCs in HO-$1^{+/+}$ and HO-$1^{-/-}$ mice (Supplemental Figure 1). However, relative to HO-$1^{+/+}$ or HBAC mice, HO-1 deficiency results in a striking decline in the proportion of DCs ($P<0.001$) and a concomitant increase in the proportion of macrophages ($P<0.001$) after IRI (Figure 4, A–C). The increase in macrophages and decrease in DCs in HO-$1^{-/-}$ kidneys was also confirmed by analyzing changes in absolute cell number in mice subjected to renal IRI (Figure 4, D and E).

HO-1–Deficient RMNCs Exhibit Dysregulated Cytokine Gene Expression

RMNCs (CD45$^+$ CD11b$^+$ MHCII$^+$ Gr-1$^-$) isolated from kidneys 1 day after IRI demonstrated robust induction of HO-1 expression compared with RMNCs isolated from sham kidneys ($P<0.001$) (Figure 5A). Cytokine expression was also assessed, which revealed marked induction of proinflammatory IL-6 expression ($P<0.05$) in HO-$1^{-/-}$ compared with HO-$1^{+/+}$ and HBAC RMNCs (Figure 5B). The expression of the proinflammatory cytokine TNFα was suppressed in HO-$1^{-/-}$ RMNCs (Figure 5C), likely as a result of decreased DCs within the RMNC population after IRI (Figures 3 and 4).[16] Interestingly, RMNCs from HBAC mice overexpress IL-10 relative to HO-$1^{+/+}$ and HO-$1^{-/-}$ RMNCs ($P<0.01$) (Figure 5D).

HO-1 Deficiency Increases Trafficking of Resident RMNCs from the Kidney after IRI

To mitigate the confounding variable of a systemic proinflammatory milieu and deranged immune system in HO-$1^{-/-}$ mice,[26,27] we employed syngeneic kidney transplant experiments, utilizing GFP$^-$ HO-$1^{+/+}$ recipients and donor kidneys from their GFP$^+$ HO-$1^{-/-}$ or GFP$^+$ HO-$1^{+/+}$ littermates (Figure 6A, Table 1). This model provides a clear means to delineate kidney-resident immune cells (GFP$^+$ CD45$^+$) from recipient-derived immune cells (GFP$^-$ CD45$^+$) that infiltrate the graft after injury, which was induced by 25 minutes of warm ischemia (Figure 6B). Flow cytometry analysis of GFP$^+$ HO-$1^{-/-}$ grafts demonstrated a significant decrease in the proportion of resident GFP$^+$ CD45$^+$ cells compared with GFP$^+$ HO-$1^{+/+}$ grafts ($P \leq 0.001$) (Figure 6C) 3 days after transplantation, supporting our previous finding (Figure 3) and suggesting increased trafficking of RMNCs from HO-$1^{-/-}$ kidneys after ischemic injury. However, there was no significant difference in the proportion of graft-infiltrating cells (GFP$^-$ CD45$^+$) in the HO-$1^{-/-}$ graft compared with the HO-$1^{+/+}$ control (Figure 6D). The vast majority of GFP$^+$ CD45$^+$ cells in

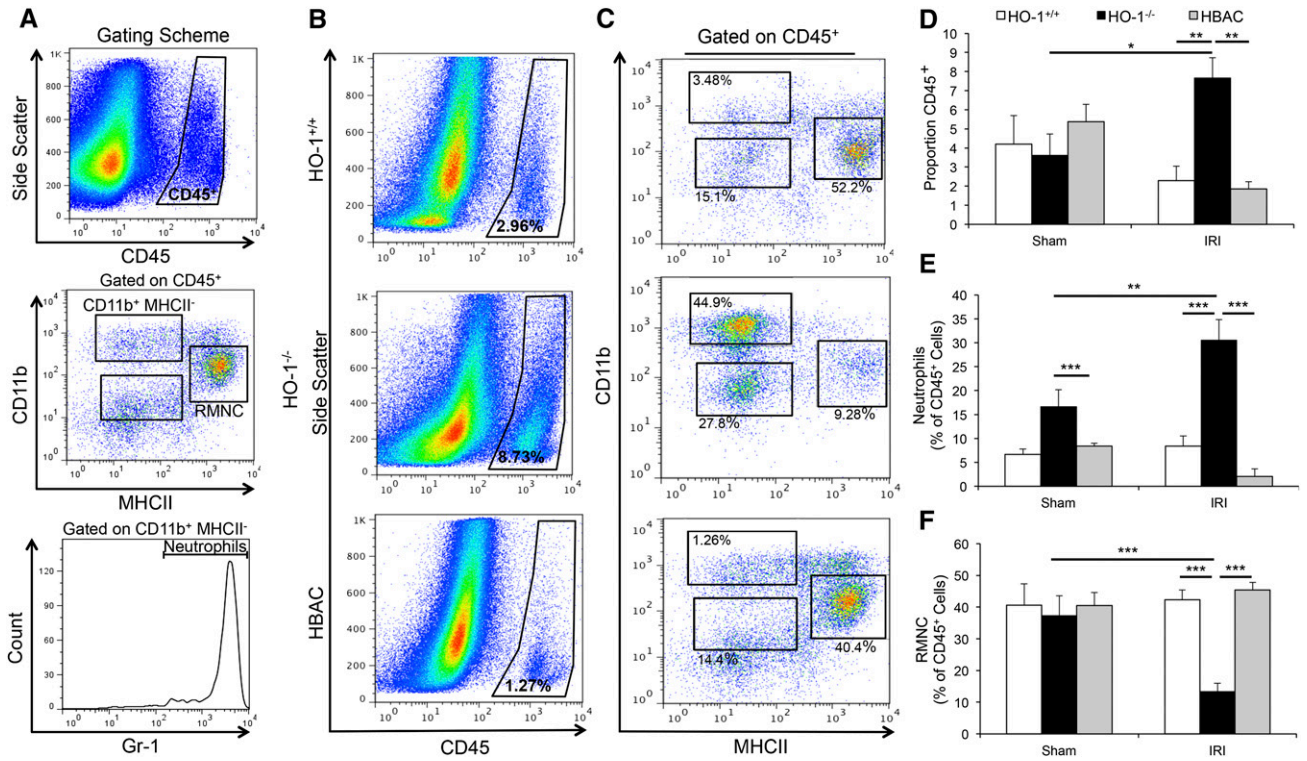

Figure 3. HO-1 deficiency alters the trafficking of myeloid-derived immune cells after IRI. One day after sham surgery or 10 minutes of bilateral IRI, kidneys are explanted and homogenized for analysis by flow cytometry. (A) Scheme depicting the sequential gating used to identify neutrophils ($CD45^+$ $CD11b^{hi}$ $MHCII^-$ $Gr\text{-}1^{hi}$) and RMNCs ($CD45^+$ $CD11b^+$ $MHCII^+$) in the kidney of $HO\text{-}1^{+/+}$, $HO\text{-}1^{-/-}$, and HBAC mice. (B and C) Representative flow cytometry histograms depicting the proportion of bone marrow–derived cells ($CD45^+$) (B) or neutrophils and RMNCs (C) in the kidney after IRI. (D) Quantification of $CD45^+$ cells in the kidney, presented as a proportion of total cells. (E and F) Quantification of neutrophils (E) and RMNCs (F) in the kidney, presented as a proportion of $CD45^+$ cells. *$P \leq 0.05$; **$P \leq 0.01$; ***$P \leq 0.001$ versus the indicated group. Results are expressed as the mean±SEM. n=4 per group.

$HO\text{-}1^{+/+}$ grafts were RMNCs (Figure 6E). The proportion of RMNCs decreased significantly in $HO\text{-}1^{-/-}$ grafts ($P \leq 0.05$), likely owing to a decrease in the resident DC population (GFP^+ $F4/80^{hi}$ $CD11b^{lo}$) ($P<0.05$) compared with $HO\text{-}1^{+/+}$ grafts (Figure 6F). The proportion of resident macrophages (GFP^+ $F4/80^{lo}$ $CD11b^{hi}$) was significantly higher in $HO\text{-}1^{-/-}$ grafts (Figure 6G).

HO-1 Deficiency Increases RMNC Trafficking to the Peripheral Lymphoid Organs

We next examined whether the decreased proportion of intrarenal resident DCs in $HO\text{-}1^{-/-}$ kidneys after IRI (Figure 4) or syngeneic transplantation (Figure 6) resulted from increased trafficking of these cells to the peripheral lymphoid organs. Kidneys from GFP^+ $HO\text{-}1^{+/+}$ or GFP^+ $HO\text{-}1^{-/-}$ mice were transplanted into GFP^- $HO\text{-}1^{+/+}$ littermates and the recipient's lymphoid organs were harvested 1 or 3 days after transplantation and subjected to flow cytometry analysis (Figure 7A). There was a significant increase in GFP^+ cells in the spleen, renal lymph nodes (LNs), and mesenteric LNs in recipients of $HO\text{-}1^{-/-}$ grafts at day 1 after transplantation (Figure 7, B and D, Supplemental Figure 2). GFP^+ cells were not detectable in the blood, thymus, or contralateral kidney of recipients transplanted with $HO\text{-}1^{+/+}$ or $HO\text{-}1^{-/-}$ grafts (data not shown), suggesting targeted migration of donor-derived immune cells to the secondary lymphoid organs of the recipients. The trend of increased migration of GFP^+ $HO\text{-}1^{-/-}$ RMNCs continued at day 3 after transplantation, but was only significant in the mesenteric LNs (Figure 7, C and D, Supplemental Figure 2A). Immunofluorescence microscopy of frozen sections from recipient spleen, renal LNs, and mesenteric LNs confirmed increased migration of $HO\text{-}1^{-/-}$ RMNCs to these tissues and revealed a specific pattern of homing of GFP^+ graft-derived cells to the T cell centers of the spleen and the periphery of the LN (Figure 7D). We also confirmed that the GFP^+ cells in these tissues are nucleated (Supplemental Figure 2B, inset) and express MHCII (Supplemental Figure 2C).

Myeloid HO-1 Deficiency Impairs Resolution of Kidney Injury Induced by IRI

To delineate the effects of HO-1 deficiency within the renal parenchyma versus the RMNC (Table 1), we utilized mice with myeloid-restricted expression of Cre-recombinase (LysM-Cre) that were bred to mice containing biallelic floxed HO-1

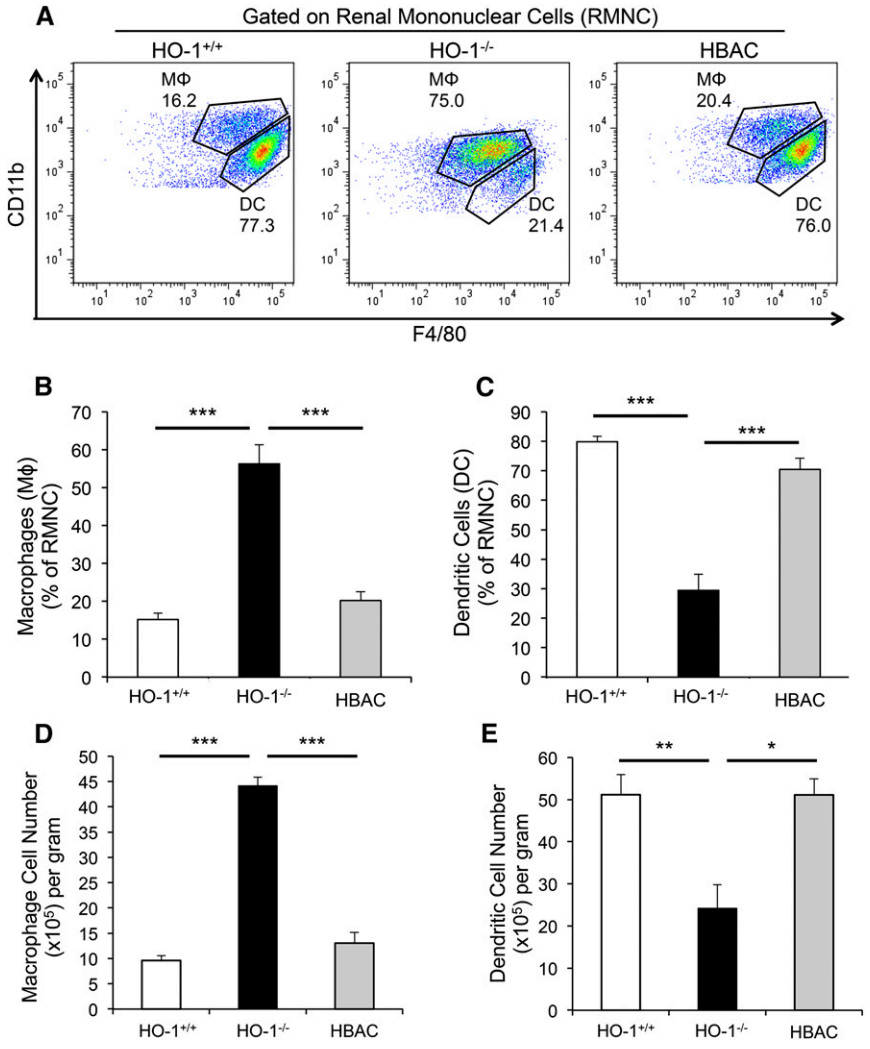

Figure 4. The intrarenal resident F4/80^{hi} CD11b^{lo} subpopulation of RMNCs specifically decreases after IRI. (A) RMNCs (intrarenal CD11b^{+} MHCII^{+}) from HO-1$^{+/+}$, HO-1$^{-/-}$, and HBAC mice subjected to IRI are further characterized based on their expression of F4/80. (B–D) F4/80^{lo} CD11b^{hi} macrophages (MΦ) (B) and F4/80^{hi} CD11b^{lo} DCs (C) are presented as a proportion of total RMNCs and as absolute cell number per gram of kidney weight for macrophages (D) and DCs (E). *$P\leq0.05$; **$P\leq0.01$; ***$P\leq0.001$ versus the indicated group. Results are expressed as the mean±SEM. n=4 per group.

constructs to generate mice with myeloid-specific HO-1 deficiency, hereafter called HO-1$^{LysM-/-}$. These mice lack HO-1 expression in cells of the myeloid lineage, which includes macrophages, monocytes, neutrophils, and tissue-resident DCs.[11,28–30] HO-1 flox mice lacking LysM-Cre (HO-1$^{LysM+/+}$) were used as controls. Twenty-five minutes of bilateral renal ischemia was sublethal (0% mortality; data not shown) but caused a significant increase in serum creatinine at days 1 and 3 in both HO-1$^{LysM-/-}$ and HO-1$^{LysM+/+}$ mice compared with baseline (Figure 8A). Compared with baseline values, serum creatinine at days 5 and 7 remained significantly elevated in HO-1$^{LysM-/-}$ mice but not HO-1$^{LysM+/+}$ control mice. Three days after IRI, cast formation, proximal tubular brush border loss, and tubule necrosis were evident but not significantly different between kidneys from HO-1$^{LysM-/-}$ and HO-1$^{LysM+/+}$ mice (Figure 8, B and C). Seven days after IRI, compared with HO-1$^{LysM+/+}$ kidneys, there were significantly more casts in HO-1$^{LysM-/-}$ kidneys (21.3±2.6 versus 5.98±1.14 in HO-1$^{LysM+/+}$, $P<0.01$; Figure 8D) and delayed regeneration of the proximal tubule brush border (Figure 8D, inset). The apparent delay in recovery from IRI in HO-1$^{LysM-/-}$ kidneys was accompanied by a striking increase in renal fibrosis, as evidenced by increased picrosirius red staining for collagen (Figure 8E) and fibronectin expression (Figure 8F).

Myeloid HO-1 Regulates Trafficking of DCs after IRI

Examination of myeloid trafficking by flow cytometry (Figure 9A) revealed a striking decrease in the RMNC subset in HO-1$^{LysM-/-}$ mice after IRI compared with controls (Figure 9B). Consistent with our previous findings, the proportion of intrarenal DCs (Figure 9, A and C) significantly decreased, whereas the proportion of macrophages significantly increased (Figure 9, A and D) after IRI in the kidney of HO-1$^{LysM-/-}$ mice compared with HO-1$^{LysM+/+}$ controls. These findings were corroborated with absolute cell counts (Supplemental Figure 3, A– C). In addition, the absolute number (Supplemental Figure 3D) but not proportion (Figure 9E) of Ly6C^{hi} proinflammatory macrophages was significantly higher in HO-1$^{LysM-/-}$ kidneys compared with controls, whereas no significant difference in neutrophil infiltration was observed (Figure 9F, Supplemental Figure 3E).

DISCUSSION

HO-1 modulates trafficking of three types of myeloid immune cells: neutrophils, macrophages, and tissue-resident DCs. First, HO-1 deficiency results in early (day 1) infiltration of neutrophils after IRI consistent with previous studies showing a role for HO-1 expression in trafficking of neutrophils.[31,32] We have shown that HO-1 overexpression in the heart prevents injury-induced neutrophil infiltration occurring secondary to myocyte dysfunction and death.[18] In this study, we demonstrate significantly increased neutrophil infiltration after AKI in HO-1$^{-/-}$ kidneys, but not in HO-1$^{LysM-/-}$ mice, which supports a protective role for

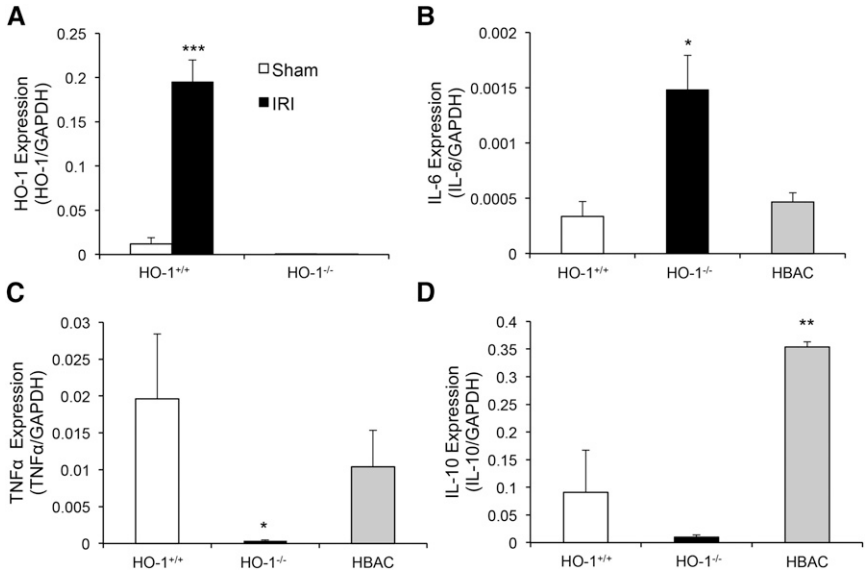

Figure 5. HO-1–deficient RMNCs exhibit dysregulated cytokine gene expression. Gene expression in electronically sorted RMNCs is analyzed by real-time PCR. (A) HO-1 expression is assessed in HO-$1^{+/+}$ and HO-$1^{-/-}$ mice subjected to sham or 10 minutes of ischemia and 1 day of reperfusion. (B–D) Expression of the cytokines IL-6 (B), TNFα (C), and IL-10 (D) is quantified in HO-$1^{+/+}$, HO-$1^{-/-}$, and HBAC RMNC 1 day after 10 minutes of renal ischemia. Analysis is performed in triplicate and results are normalized to GAPDH and expressed as the mean±SEM. *P≤0.05; **P≤0.01; ***P≤0.001. n=3 per group.

HO-1 against neutrophil infiltration at the level of the tissue parenchyma.

Although many studies have described the protection conferred upon parenchymal cells by HO-1 expression, relatively few have used targeted approaches such as cell tracking and cell-specific transgenic mice to specifically delineate the effects of myeloid HO-1 expression. One such study showed that myeloid-specific ablation of HO-1 results in activation of antigen-presenting cells and the adaptive immune system in experimental autoimmune encephalomyelitis.[28] Another study showed that myeloid HO-1 expression is necessary for proinflammatory macrophage skewing in the adipose tissue of mice on a high-fat diet.[30] In this study, HO-1 expression appears to be important within intrarenal resident DCs and infiltrating macrophages.

At day 3, transplant experiments with HO-$1^{-/-}$ renal grafts (HO-$1^{-/-}$ renal parenchyma and RMNCs, but HO-$1^{+/+}$ systemic immune system; Table 1) demonstrate a significant decrease in resident (GFP^+) DCs, yet no significant increase in the infiltration of monocyte-derived macrophages from the circulation (GFP^-). However, HO-$1^{LysM-/-}$ mice (HO-$1^{-/-}$ myeloid cells, including RMNCs, but HO-$1^{+/+}$ renal parenchyma; Table 1) subjected to IRI exhibit a significant decrease of DCs and a significant increase in $Ly6C^+$ proinflammatory macrophages 3 days after IRI. These results argue that myeloid HO-1 regulates DC emigration and directly modulates the macrophage response to AKI, independent of HO-1 expression in the renal parenchyma. In addition, we observed no significant differences in serum creatinine or tubulointerstitial damage between HO-$1^{LysM-/-}$ and HO-$1^{LysM+/+}$ mice 3 days after IRI, which suggests that these effects on myeloid trafficking are independent of the extent of tissue injury and subsequent functional changes. However, at later time points (*e.g.*, day 7), myeloid HO-1 deficiency impairs the resolution of renal injury, resulting in increased renal fibrosis, persistence of tubular casts, and delayed regeneration of the proximal tubule brush border. Collectively, these data suggest that myeloid HO-1 expression is important in regulating the early (*e.g.*, day 3) trafficking of DCs from and macrophages to the kidney after AKI, and that these events have an important effect at later time points in the resolution of kidney injury.

Injury-induced emigration of DCs from HO-$1^{-/-}$ kidneys could be explained by at least three possibilities. First, increased renal parenchymal injury in HO-$1^{-/-}$ mice could lead to hyperactivation of intrarenal resident DCs, thus increasing their trafficking to the peripheral lymphoid organs. Second, as previously described,[27] the systemic proinflammatory milieu in HO-$1^{-/-}$ mice could effectively prime DCs in the quiescent kidney to be more likely to emigrate after injury. Finally, HO-1 deficiency in DCs could have an effect on migratory capacity, resulting in increased trafficking secondary to IRI. To address each of these possibilities, we used myeloid-specific HO-$1^{-/-}$ mice and syngeneic transplant experiments with HO-$1^{+/+}$ recipient mice. Regarding the first possibility, we confirmed previous findings demonstrating that the mild ischemia time (10 minutes) causes significant injury in HO-$1^{-/-}$ mice without causing significant changes in HO-$1^{+/+}$ mice.[33] This raises the possibility that our finding of DC emigration after 10 minutes of IRI, which only occurred in HO-$1^{-/-}$ kidneys, may simply result from significantly less AKI in HO-$1^{+/+}$ mice. In subsequent studies utilizing HO-$1^{LysM-/-}$ mice, 25 minutes of bilateral ischemia induced significant changes in serum creatinine at day 1 and 3 compared to baseline levels. In these studies, although the extent of injury was no different between HO-$1^{LysM-/-}$ mice and HO-$1^{LysM+/+}$ controls, significant DC emigration and macrophage infiltration was still evident in HO-$1^{LysM-/-}$ kidneys. This observation suggests that our earlier findings are specific to HO-1 expression in RMNCs and circulating myeloid cells, as opposed to the extent of AKI.

We have also provided evidence suggesting that the second possibility is unlikely. After syngeneic kidney transplantation, increased DC emigration from the graft is observed in HO-$1^{-/-}$ kidneys compared to HO-$1^{+/+}$ grafts. Because the recipients in

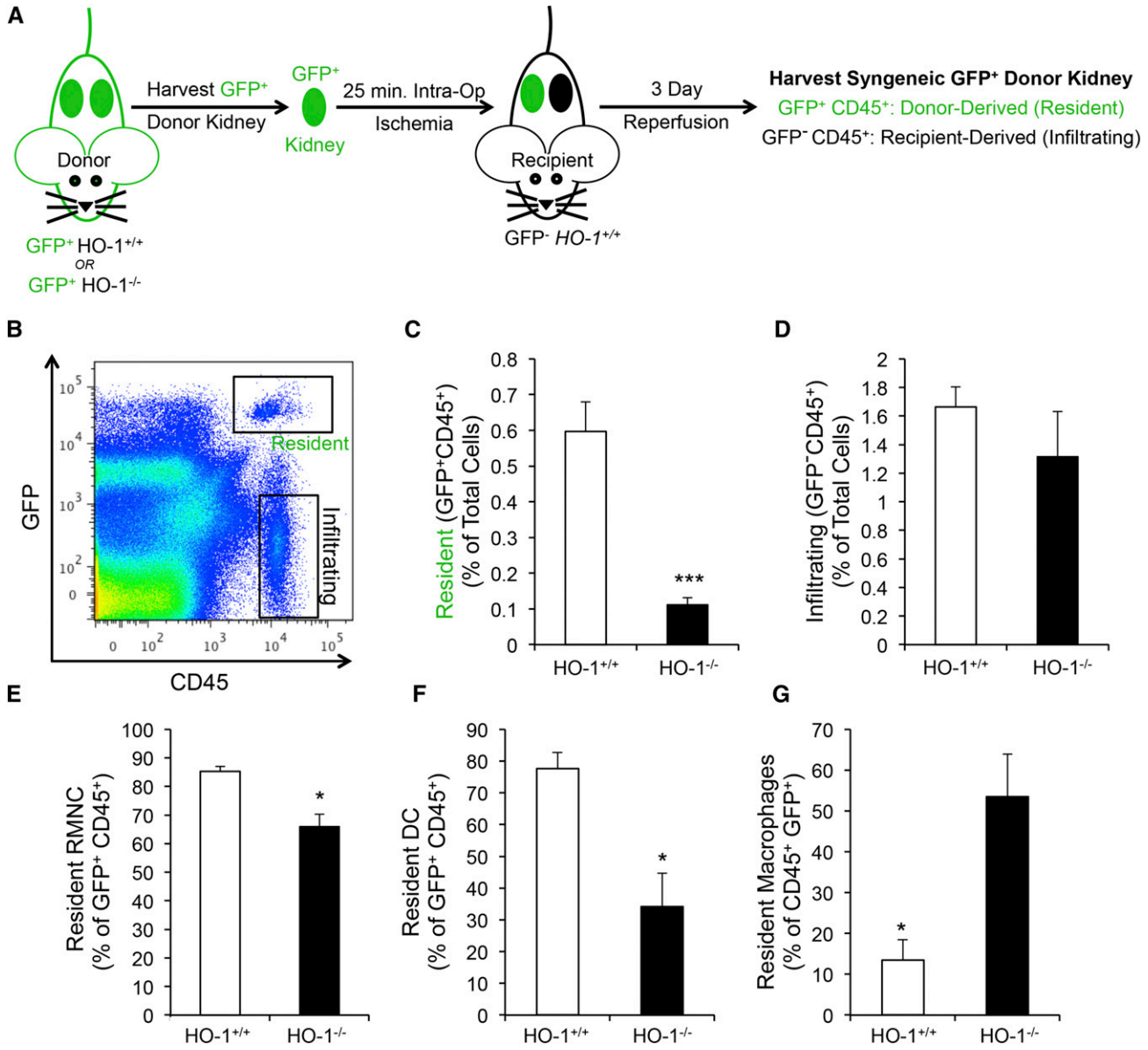

Figure 6. The resident RMNC population declines in HO-1$^{-/-}$ kidneys after IRI induced by syngeneic transplantation. (A) HO-1$^{-/-}$ or HO-1$^{+/+}$ kidneys are harvested from GFP^{+} donors and transplanted into GFP^{-} HO-1$^{+/+}$ littermates. IRI is modeled by 25 minutes of intraoperative ischemia. (B) Grafts are harvested 3 days after transplantation and analyzed by flow cytometry for the emigration of GFP^{+} CD45^{+} donor-derived resident cells or infiltration of GFP^{-} CD45^{+} recipient-derived inflammatory cells. (C and D) Emigration of GFP^{+} CD45^{+} donor-derived cells (C) and infiltration of GFP^{-} CD45^{+} recipient-derived cells (D), expressed as a proportion of the total renal cell population. (E–G) Donor-derived intrarenal resident cells are further characterized as CD11b^{+} MHCII^{+} RMNCs (E), F4/80^{hi} CD11b^{lo} DCs (F), or F4/80^{lo} CD11b^{hi} macrophages (G) and expressed as a proportion of GFP^{+} CD45^{+} cells. *P<0.05; ***P≤0.001. n=3 per group. Results are expressed as the mean±SEM.

the transplant experiments are HO-1$^{+/+}$, the effect of the systemic proinflammatory milieu in HO-1$^{-/-}$ mice is nullified, thus allowing for the isolation of events that are caused by IRI in the HO-1–deficient renal parenchyma or resident RMNC network. Our findings support previous studies that utilized pharmacologic modulation of HO-1 expression to demonstrate a role for HO-1 in immune cell trafficking.[34,35] Collectively, these findings support a role for myeloid HO-1 in regulating the trafficking of intrarenal resident DCs (the third possibility). Although the decrease in intrarenal DCs could also be the result of a phenotypic switch, whereby DCs acquire the phenotypic characteristics of renal macrophages by reciprocally regulating their expression of CD11b and F4/80, this possibility is less likely, because syngeneic transplant experiments confirm increased DC emigration from the kidney to the peripheral lymphoid organs.

Table 1. Mouse models of HO-1 expression

Mouse/Model[a]	HO-1 Expression	Use
HO-1$^{-/-}$	Global HO-1 deficiency	Role of HO-1 in regulating the global response to IRI
HBAC	Global overexpression of HO-1	Protection against IRI in humanized HO-1 overexpressing mice
Syngeneic transplant of HO-1$^{+/+}$ recipient with HO-1$^{+/+}$ or HO-1$^{-/-}$ graft	HO-1–deficient renal parenchyma and RMNCs, HO-1$^{+/+}$ systemic immune response	Role of HO-1 in renal parenchyma and RMNCs, in the context of a normal systemic inflammatory milieu; cell trafficking
HO-1$^{LysM-/-}$	HO-1–deficient RMNCs and myeloid systemic immune response, HO-1$^{+/+}$ renal parenchyma	Role of HO-1 in RMNCs and myeloid systemic inflammatory response

[a]For control strains, see the text.

It is important to note technical differences between our experiments utilizing 25 minutes of bilateral IRI and those using syngeneic transplantation. In both instances, the warm ischemia time was carefully controlled and limited to precisely 25 minutes. In addition, the ensuing inflammatory response in both models was sterile in nature. Using inbred mouse strains and littermates as donor/recipient pairs in the transplant experiments eliminated the potential of a confounding alloresponse. However, several inherent differences exist, and deserve mention. First, transplant surgery is technically more complex than IRI surgery. Blood flow through the aorta and inferior vena cava just proximal to the bifurcation is stopped briefly during the vascular anastomosis. In addition, although the right kidney is removed during the transplant procedure, modeling bilateral IRI is not possible in the transplant model. Although these considerations may cause slight variations in the systemic immune response, their effect on our experimental observations is expected to be minimal.

Even mild 10-minute ischemic insult had a clear effect on HO-1$^{+/+}$ mice at the level of the RMNC, as evidenced by robust induction of HO-1 expression (Figure 6). Further gene expression studies in RMNCs after IRI demonstrated several interesting findings. As expected, and consistent with previous studies, expression of the proinflammatory cytokine IL-6 was significantly elevated in HO-1$^{-/-}$ mice.[33] The finding of decreased TNFα expression in the RMNCs of HO1$^{-/-}$ mice after IRI is consistent with our finding of DC emigration from the kidney, because resident DCs are the primary source of this proinflammatory cytokine in AKI.[16] Overexpression of IL-10 in RMNCs sorted from HBAC mice is likely associated with HO-1 overexpression in these mice, because the production of anti-inflammatory IL-10 appears to be tightly coupled and proportional to HO-1 expression levels.[14,22,36]

DCs are the most abundant RMNCs in the quiescent kidney and are distributed throughout the parenchyma as an interconnected network of cells that likely contribute to tissue homeostasis and serve as sentinels to tissue insult.[24,25,37] Macrophage depletion at the time of IRI ameliorates injury, whereas its depletion later between days 3 and 5 impairs the healing process, thus highlighting the phenotypic and functional shift that occurs temporally after the induction of the inflammatory process by injury.[38,39] Thus, targeting HO-1, which we have demonstrated to be a key modulator of myeloid cell trafficking, to regulate the temporal dynamics of the myeloid inflammatory response after renal IRI and after renal transplantation is a novel and promising therapeutic target. Inhibiting the early migration of RMNCs could be a potential therapeutic approach to blunt AKI caused by IRI or graft immunogenicity in the post-transplant setting. Future studies are needed to investigate the effect of HO-1 on DC emigration after renal ischemic injury in the context of allogeneic kidney transplantation.

CONCISE METHODS

Animals

Male mice aged between 8 and 12 weeks were utilized in all experiments (Table 1). Three transgenic lines were used for experiments with 10 minutes of bilateral IRI: (*1*) global HO-1–deficient mice (HO-1$^{-/-}$) on a C57BL/6×FVB background,[40] (*2*) their HO-1$^{+/+}$ (wild-type) littermates, and (*3*) humanized HO-1 transgenic mice (HBAC) on a C57BL/6×FVB background.[22] Three transgenic lines in the same background strain were used for syngeneic kidney transplantation experiments. C57BL/6 mice expressing GFP under control of the human ubiquitin C promoter were purchased from The Jackson Laboratory (strain C57BL/6-Tg[UBC-GFP]30Scha/J; Bar Harbor, ME;). GFP$^+$ mice were bred with HO-1$^{+/-}$ mice to generate GFP$^+$ HO-1$^{+/+}$ and GFP$^+$ HO-1$^{-/-}$ littermates that were used as kidney donors. Recipients were GPF$^-$ HO-1$^{+/+}$ littermates of the donor animals.[20] Littermates from this inbred strain were used to ensure histocompatibility in syngeneic kidney transplant experiments. Two transgenic lines were used for experiments with 25 minutes of bilateral IRI: (*1*) myeloid-specific HO-1$^{-/-}$ mice (referred to as HO-1$^{LysM-/-}$) express myeloid-restricted Cre-recombinase (LysM-Cre) and biallelic floxed HO-1 constructs, and (*2*) HO-1 flox mice that lack the LysM-Cre construct (HO-1$^{LysM+/+}$) were used as controls.[30] Animal care and manipulations for experimentation were conducted in accordance with the Guide for the Care and Use of Laboratory Animals and with approval of the University of Alabama at Birmingham (UAB) Institutional Animal Care and Use Committee.

Ischemia-Reperfusion Surgery

Mice were anesthetized with isoflurane (2.5% for induction, 1.5% for maintenance). After bilateral flank incision, both renal pedicles were

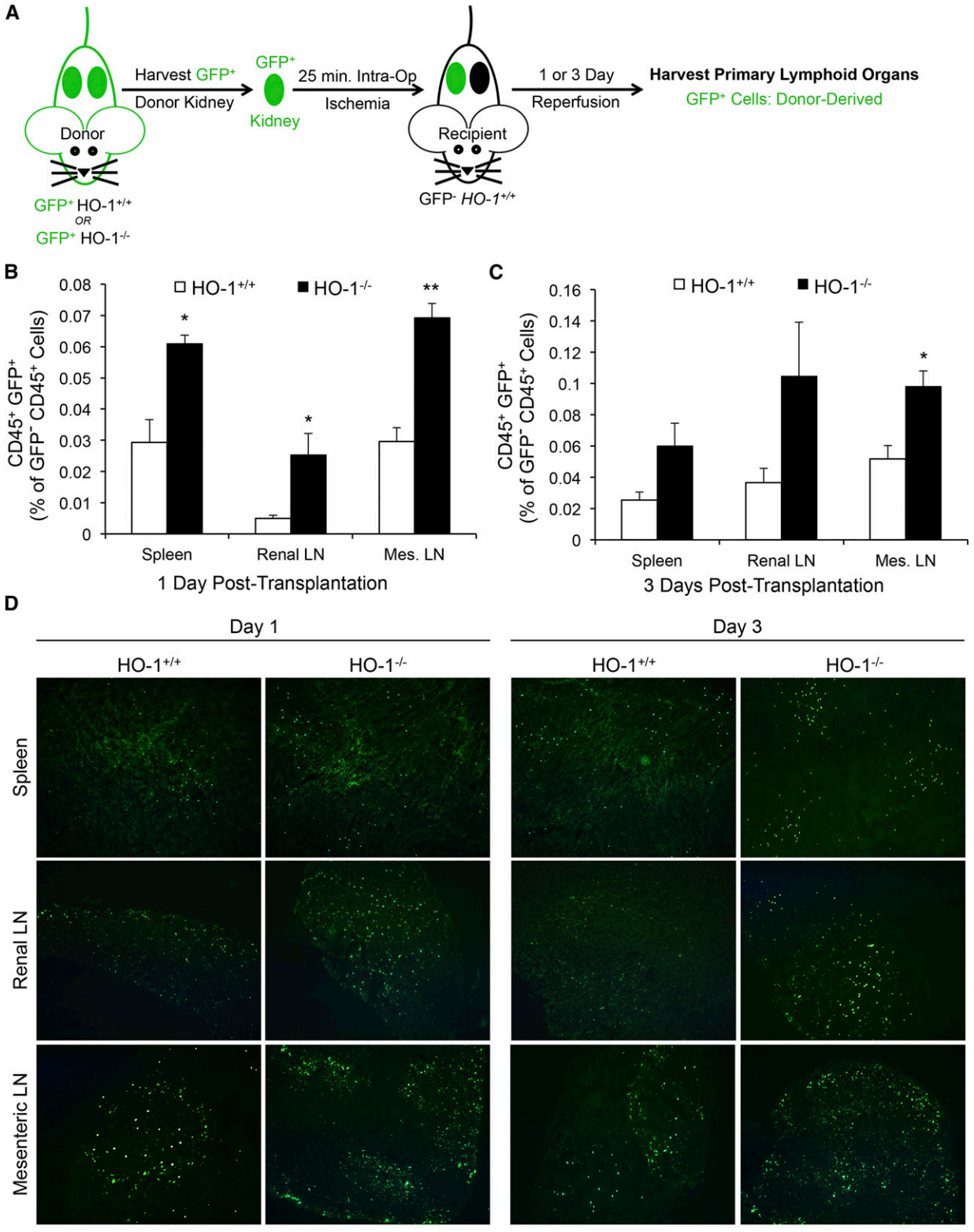

Figure 7. HO-1$^{-/-}$ RMNCs exhibit increased trafficking to the peripheral lymphoid organs. (A) RMNC trafficking is tracked using flow cytometry after syngeneic transplantation of GFP^{+} HO-1$^{-/-}$ or GFP^{+} HO-1$^{+/+}$ donor kidneys. (B and C) One day (B) or 3 days (C) after transplantation, the spleen, renal LNs, and mesenteric (Mes.) LNs are harvested from kidney transplant recipients and donor-derived RMNCs that had emigrated from the graft are identified as GFP^{+} CD45^{+}. (D) Increased trafficking from HO-1$^{-/-}$ grafts is confirmed in frozen tissue sections from the spleen, renal LNs, and mesenteric LNs from transplant recipients, utilizing the GFP^{+} signal from donor-derived RMNCs. *$P \leq 0.05$; **$P \leq 0.01$. $n=3$ per group. Results are expressed as the mean±SEM.

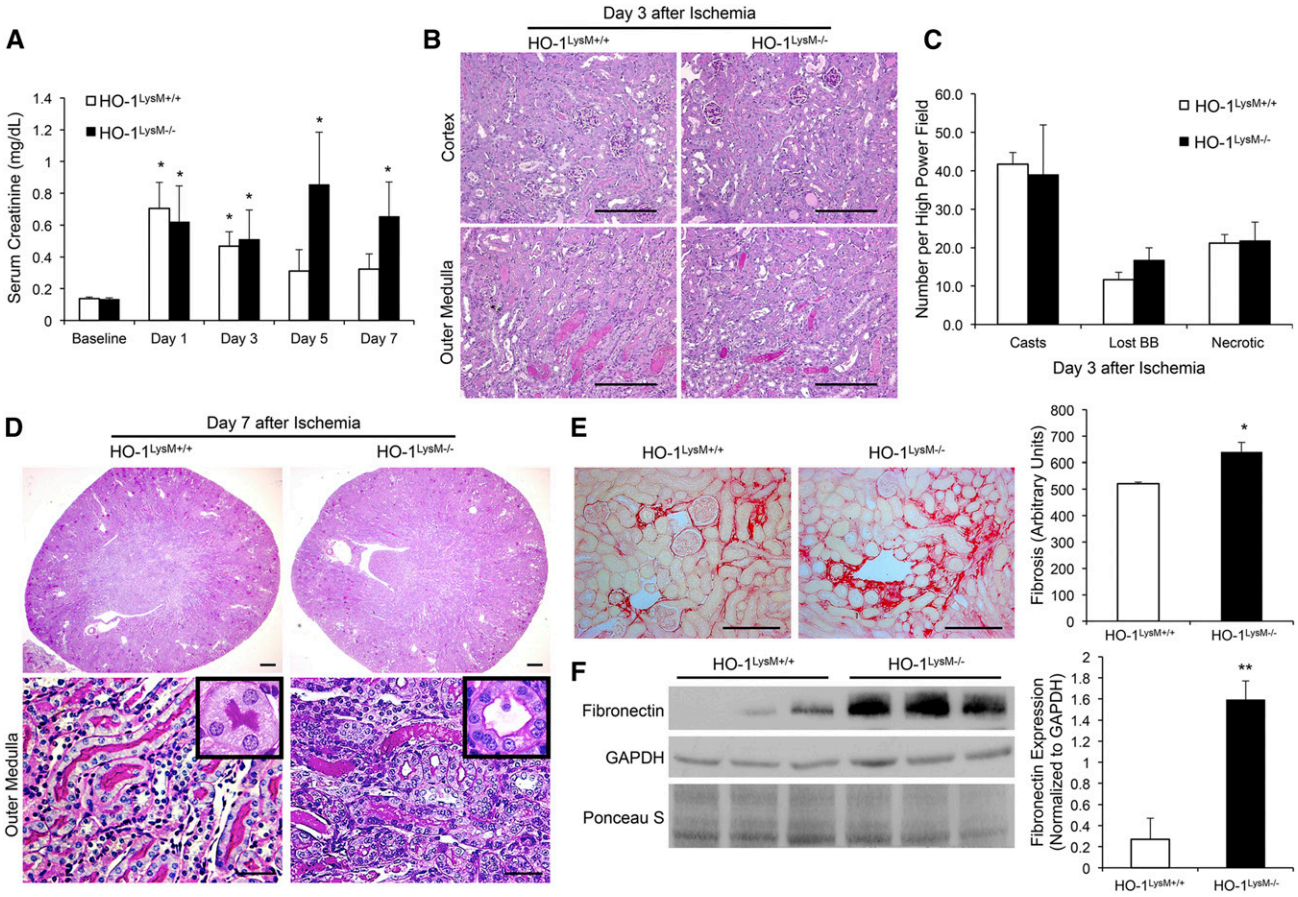

Figure 8. Myeloid HO-1 deficiency impairs resolution of kidney injury caused by IRI. Myeloid-restricted HO-1–deficient mice (HO-1$^{LysM-/-}$) and controls (HO-1$^{LysM+/+}$) are subjected to 25 minutes of bilateral IRI. (A) Serum creatinine (in milligrams per decaliter) is measured before (baseline) and at days 1, 3, 5, and 7 after IRI. (B) Representative micrographs of PAS-stained sections in the renal cortex (top) and outer medulla (bottom) of HO-1$^{LysM-/-}$ mice and HO-1$^{LysM+/+}$ controls 3 days after IRI. (C) Cast formation, loss of the brush border, and necrotic tubules are quantified in the proximal tubules of the outer medulla. Results are expressed as an average of the total number counted per high-power field at ×200 total magnification and are presented as the mean±SEM. Five images are analyzed per mouse. *n*=4 per group. (D) Representative micrographs of PAS-stained kidney cross-sections (top) and outer medulla (bottom) of HO-1$^{LysM-/-}$ mice and HO-1$^{LysM+/+}$ controls 7 days after IRI. Inset shows a single tubule at high magnification. (E) Picrosirius red staining and quantitation of collagen in representative kidney sections from HO-1$^{LysM-/-}$ and controls (HO-1$^{LysM+/+}$) 7 days after IRI. *n*=3–4 per group. (F) Western blot analysis and densitometry for fibronectin 7 days after IRI. GAPDH is used as a loading control and for normalization of densitometry values. Ponceau S staining of the membrane is also shown. *n*=3 per group. *$P \leq 0.05$; **$P \leq 0.01$. PAS, periodic acid–Schiff; BB, brush border. Bar, 200 μm in B and D; 100 μm in E.

cross-clamped for 10 or 25 minutes using an atraumatic vascular clamp (catalog number 18055-05; Fine Science Tools, Foster City, CA). Immediate blanching of the kidney confirmed ischemic induction. Body temperature was maintained at 37°C during surgery and ischemia time. Kidneys were inspected for color change within 1 minute of clamp removal to ensure uniform reperfusion. Control mice were subjected to sham operation, wherein both kidney pedicles were exposed but not clamped. Renal function was assessed by serum creatinine levels that were measured as previously described using liquid chromatography coupled to tandem mass spectrometry.[29]

Syngeneic Kidney Transplantation Model

All mice used in transplant experiments were littermates from the same inbred colony to ensure syngeneic transplantation. Donors were GFP$^+$ HO-1$^{+/+}$ or GFP$^+$ HO-1$^{-/-}$ and, in all experiments, recipients were GFP$^-$ HO-1$^{+/+}$. Orthotopic kidney transplantation was performed as previously described using the University of Alabama at Birmingham-University of California San Diego (UCSD) O'Brien Center Resource for preclinical studies (details in the Supplemental Methods).[41] The donor mouse was perfused with saline to removed intravascular immune cells. Intraoperative warm ischemia time was held constant at 25 minutes for each transplant.

Western Blot Analyses

Western blotting was performed as previously described.[18] Briefly, kidneys were homogenized in RIPA buffer (50 mmol/L Tris/HCl, 1% NP-40, 0.25% deoxycholic acid, 150 mmol/L NaCl, 1 mmol/L EGTA, 1 mmol/L sodium orthovanadate, and 1 mmol/L sodium

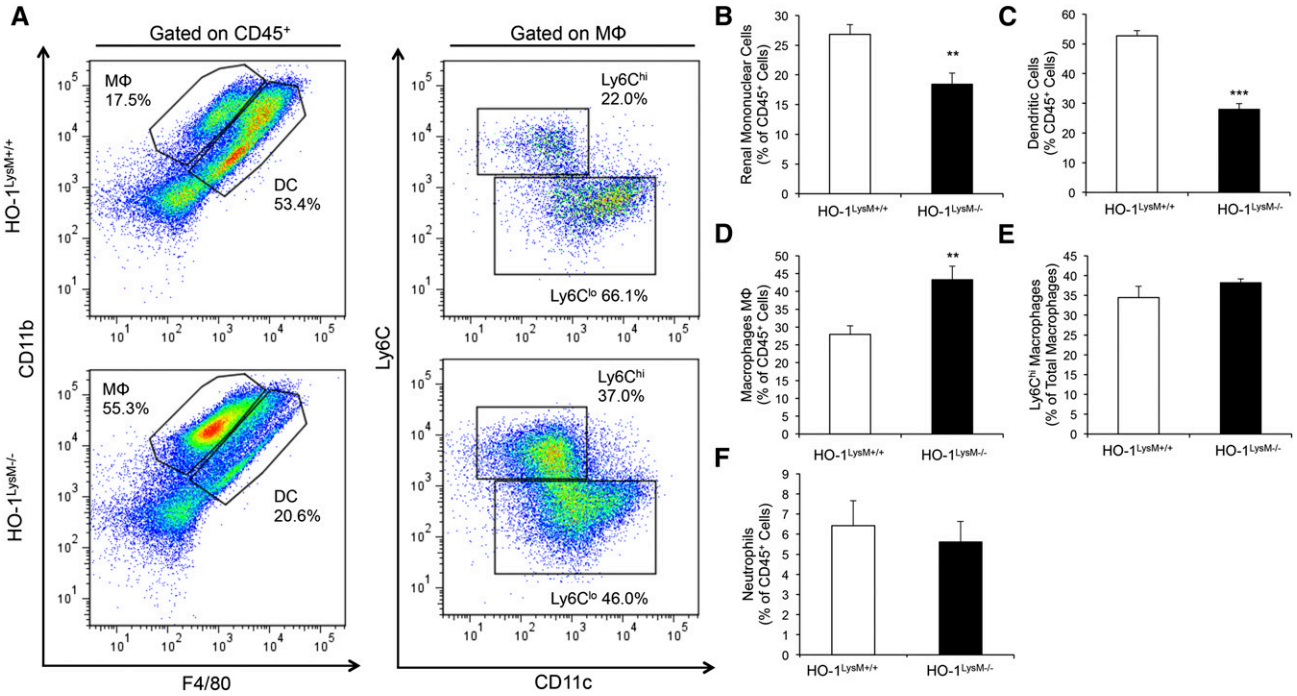

Figure 9. Myeloid HO-1 deficiency recapitulates the RMNC trafficking phenotype of global HO-1–deficient mice. Representative flow cytometry histograms (A) depicting the gating scheme for the proportional quantification of RMNCs ($CD11b^+$ $MHCII^+$) (B), DCs ($F4/80^{hi}$ $CD11b^{lo}$) (C), macrophages (MΦ; $F4/80^{lo}$ $CD11b^{hi}$) (D), $Ly6C^{hi}$ (inflammatory) macrophages (E), and neutrophils ($Gr\text{-}1^{hi}$ $CD11b^{hi}$ $MHCII^-$) (F) 3 days after 25 minutes of bilateral ischemia. Data are presented as the proportion of the parent subset (n=7–8 per group). $^{**}P \leq 0.01$; $^{***}P \leq 0.001$. Results expressed as the mean±SEM.

fluoride) with protease inhibitor (Sigma-Aldrich) and were quantified using bicinchoninic acid protein assay (Thermo Fisher Scientific). Seventy-five micrograms of protein was resolved on a 12% Tris-glycine SDS-polyacrylamide electrophoresis gel and transferred to a polyvinylidene fluoride membrane (EMD Millipore). Membranes were blocked with 5% nonfat dry milk in PBS with Tween for 1 hour and then incubated with rabbit anti-HO-1 (1:2000; Enzo Life Sciences), anti-fibronectin (1:10,000; Sigma-Aldrich), or mouse anti-smooth muscle actin (1:5000; Sigma-Aldrich) antibodies, followed by a peroxidase-conjugated goat anti-rabbit (or mouse) IgG antibody (1:10,000; Jackson ImmunoResearch Laboratories). Horseradish peroxidase activity was detected using the enhanced chemiluminescence detection system (GE Healthcare). The membrane was stripped and probed with anti-glyceraldehyde 3-phosphate dehydrogenase (GAPDH) antibody (1:5000; Sigma-Aldrich) to confirm loading and transfer. Densitometry analysis was performed and results were normalized to GAPDH expression.

Light Microscopy

For histologic analysis, kidneys were cut transversely, fixed in 10% neutral buffered formalin overnight (Fisher Fisher Scientific, Pittsburgh, PA), and stored in 70% ethanol. After paraffin embedding, 5-μm sections were stained with picrosirius red or periodic acid–Schiff, as previously described.[41,42] For the measurement of collagen deposition using picrosirius red, kidney sections were deparaffinized with xylene and then rehydrated in water through graded ethanol. The sections were incubated in picrosirius red for 1 hour followed by two washes in acidified water. The sections were then dehydrated, cleared, and mounted in a resinous medium. The area of collagen deposition, stained red by picrosirius red, was measured by color image analysis software (Image-Pro Plus; Media Cybernetics). To assess tubule injury and cast formation, kidney sections were stained with periodic acid–Schiff. Casts, loss of the brush border, and necrotic tubules were counted by a reviewer blinded to the different groups in proximal tubules of the outer medulla and are expressed as a total number per field. All proximal tubules (>80) per high-power field (×200 total magnification) were counted. At least five images were analyzed per mouse (n=4 per group).

Isolation and Enrichment of Renal Leukocytes for Flow Cytometry

Leukocytes were isolated as previously described with minor modifications, and details are included in the Supplemental Methods.[18] Kidney preparations that were electronically sorted for quantification of gene expression by real-time PCR were enriched by density gradient centrifugation using NycoPrep 1.077 density gradient solution (Axis-Shield PoC, Oslo, Norway). Cells were then stained with fluorochrome-conjugated antibodies for 30 minutes on ice for analysis by flow cytometry. Isotype-matched, fluorescently conjugated antibodies of irrelevant specificity were used as controls. Results were analyzed using FlowJo Software (Tree Star Inc., Ashland, OR). The absolute cell numbers were determined using AccuCheck Counting Beads.[43]

Table 2. Primer sequences used in real-time PCR analysis

Gene	Primer Sequence (5′– 3′)
HO-1 Fwd	ggtgatggcttccttgtacc
HO-1 Rev	agtgaggcccataccagaag
GAPDH Fwd	atcatccctgcatccact
GAPDH Rev	atccacgacggacacatt
TNFα Fwd	acggcatggatctcaaagac
TNFα Rev	agatagcaaatcggctgacg
IL-6 Fwd	ctgcaagagacttccatccag
IL-6 Rev	agtggtatagacaggtctgttgg
IL-10 Fwd	gctcttactgactggcatgag
IL-10 Rev	cgcagctctaggagcatgtg

Fwd, forward; Rev, reverse.

Immunofluorescence Microscopy

Tissues harvested from mice transplanted with GFP^+ kidneys that were used for immunofluorescence studies were cut in transverse section, fixed in 2% paraformaldehyde for 2 hours at 4ºC, and then cryopreserved in 20% sucrose solution at 4ºC for 2 days. The tissues were then embedded in Optimal Cutting Temperature freezing media and stored at −80ºC. Five-micrometer sections were cut, mounted on slides, washed in PBS at room temperature, mounted with media that contained 4′,6-diamidino-2-phenylindole, and imaged. The stained sections were imaged on an epifluorescence microscope (Leica DMIRB) with Image-Pro 5.1 software (Media Cybernetics). Confocal images were captured using a Leica TCS-SP5 confocal microscope.

Real-Time PCR Analysis

RMNCs ($CD45^+CD11b^+MHCII^+Gr\text{-}1^+$) from mice subjected to IRI or sham surgery were isolated and collected on a FACSAria cell sorter (BD Biosciences) as described above. Total RNA was isolated from the sorted cells using TRIzol reagent (Invitrogen) according to the manufacturer's protocol. One microgram of total RNA was converted to cDNA using the QuantiTect Reverse Transcription Kit (Qiagen). Quantitative real-time PCR was performed with SYBR Green Master Mix (Invitrogen) and 10 pmol of primers. Primer sequences (5′–3′) are provided in Table 2 as previously described.[18] Relative gene expression was normalized to mouse GAPDH as an internal control and quantified using the $\Delta\Delta$ threshold cycle method. Samples were performed in triplicate.

Statistical Analyses

Data are presented as the mean±SEM. The *t* test was used for comparison between two groups. Changes in serum creatinine values at days 1, 3, 5, and 7 after 25 minutes of bilateral IRI were compared with baseline levels using a paired *t* test of log-transformed values. ANOVA and the Newman–Keuls post test were used for analyses comparing more than two groups. Differences were considered statistically significant at $P<0.05$.

ACKNOWLEDGMENTS

We thank the UAB Comprehensive Flow Cytometry Core for assistance with flow cytometry. We appreciate the technical assistance of Reny Joseph, Amie Traylor, and Daniel McFalls. We also thank Dr. Harald Esterbauer for the HO-$1^{LysM-/-}$ mice.

This work was supported by grants from the National Institutes of Health (NIH) (R01-DK59600 to A.A., R01-DK083390 to J.F.G. and A.A., and T32-DK7545 to S.B.), the core resource of the UAB-UCSD O'Brien Center (P30-DK079337 to A.A.), and the American Heart Association (13PRE17000013 to T.D.H. and 11POST7600074 to S.B.), as well as a fellowship from the International Society of Nephrology (to A.I.K.). L.M. Curtis is supported by a Department of Veterans Affairs Career Development Grant (1K2-BX001581) from the Office of Research and Development, Medical Research Service, Department of Veterans Affairs. The UAB Comprehensive Flow Cytometry Core is funded by grants from the NIH (P30-AR048311 and P30-AI027767).

This work was selected for an oral presentation at the 2014 Annual Meeting of the American Society of Nephrology, November 11–16, 2014, in Philadelphia, Pennsylvania.

DISCLOSURES

None.

REFERENCES

1. Kaushal GP, Shah SV: Challenges and advances in the treatment of AKI. *J Am Soc Nephrol* 25: 877–883, 2014
2. Chawla LS, Eggers PW, Star RA, Kimmel PL: Acute kidney injury and chronic kidney disease as interconnected syndromes. *N Engl J Med* 371: 58–66, 2014
3. Guo JK, Cantley LG: Cellular maintenance and repair of the kidney. *Annu Rev Physiol* 72: 357–376, 2010
4. Kapitsinou PP, Sano H, Michael M, Kobayashi H, Davidoff O, Bian A, Yao B, Zhang MZ, Harris RC, Duffy KJ, Erickson-Miller CL, Sutton TA, Haase VH: Endothelial HIF-2 mediates protection and recovery from ischemic kidney injury. *J Clin Invest* 124: 2396–2409, 2014
5. Li L, Okusa MD: Macrophages, dendritic cells, and kidney ischemia-reperfusion injury. *Semin Nephrol* 30: 268–277, 2010
6. Li L, Huang L, Ye H, Song SP, Bajwa A, Lee SJ, Moser EK, Jaworska K, Kinsey GR, Day YJ, Linden J, Lobo PI, Rosin DL, Okusa MD: Dendritic cells tolerized with adenosine A_2AR agonist attenuate acute kidney injury. *J Clin Invest* 122: 3931–3942, 2012
7. Huen SC, Cantley LG: Macrophage-mediated injury and repair after ischemic kidney injury [published online ahead of print January 19, 2014]. *Pediatr Nephrol* doi:10.1007/s00467-013-2726-y
8. Cooper JE, Wiseman AC: Acute kidney injury in kidney transplantation. *Curr Opin Nephrol Hypertens* 22: 698–703, 2013
9. Kim BS, Lim SW, Li C, Kim JS, Sun BK, Ahn KO, Han SW, Kim J, Yang CW: Ischemia-reperfusion injury activates innate immunity in rat kidneys. *Transplantation* 79: 1370–1377, 2005
10. Ojo AO, Wolfe RA, Held PJ, Port FK, Schmouder RL: Delayed graft function: Risk factors and implications for renal allograft survival. *Transplantation* 63: 968–974, 1997
11. Fukazawa K, Lee HT: Volatile anesthetics and AKI: Risks, mechanisms, and a potential therapeutic window. *J Am Soc Nephrol* 25: 884–892, 2014
12. White LE, Hassoun HT: Inflammatory mechanisms of organ crosstalk during ischemic acute kidney injury. *Int J Nephrol* 2012: 505197, 2012
13. Lech M, Gröbmayr R, Ryu M, Lorenz G, Hartter I, Mulay SR, Susanti HE, Kobayashi KS, Flavell RA, Anders HJ: Macrophage phenotype controls long-term AKI outcomes—kidney regeneration versus atrophy. *J Am Soc Nephrol* 25: 292–304, 2014

14. Hull TD, Agarwal A, George JF: The mononuclear phagocyte system in homeostasis and disease: A role for heme oxygenase-1. *Antioxid Redox Signal* 20: 1770–1788, 2014
15. Nath KA: Heme oxygenase-1: A provenance for cytoprotective pathways in the kidney and other tissues. *Kidney Int* 70: 432–443, 2006
16. Dong X, Swaminathan S, Bachman LA, Croatt AJ, Nath KA, Griffin MD: Resident dendritic cells are the predominant TNF-secreting cell in early renal ischemia-reperfusion injury. *Kidney Int* 71: 619–628, 2007
17. Nath KA: Heme oxygenase-1 and acute kidney injury. *Curr Opin Nephrol Hypertens* 23: 17–24, 2014
18. Hull TD, Bolisetty S, DeAlmeida AC, Litovsky SH, Prabhu SD, Agarwal A, George JF: Heme oxygenase-1 expression protects the heart from acute injury caused by inducible Cre recombinase. *Lab Invest* 93: 868–879, 2013
19. Dong X, Swaminathan S, Bachman LA, Croatt AJ, Nath KA, Griffin MD: Antigen presentation by dendritic cells in renal lymph nodes is linked to systemic and local injury to the kidney. *Kidney Int* 68: 1096–1108, 2005
20. Park DJ, Agarwal A, George JF: Heme oxygenase-1 expression in murine dendritic cell subpopulations: Effect on CD8+ dendritic cell differentiation in vivo. *Am J Pathol* 176: 2831–2839, 2010
21. Rémy S, Blancou P, Tesson L, Tardif V, Brion R, Royer PJ, Motterlini R, Foresti R, Painchaut M, Pogu S, Gregoire M, Bach JM, Anegon I, Chauveau C: Carbon monoxide inhibits TLR-induced dendritic cell immunogenicity. *J Immunol* 182: 1877–1884, 2009
22. Kim J, Zarjou A, Traylor AM, Bolisetty S, Jaimes EA, Hull TD, George JF, Mikhail FM, Agarwal A: In vivo regulation of the heme oxygenase-1 gene in humanized transgenic mice. *Kidney Int* 82: 278–291, 2012
23. Pittock ST, Norby SM, Grande JP, Croatt AJ, Bren GD, Badley AD, Caplice NM, Griffin MD, Nath KA: MCP-1 is up-regulated in unstressed and stressed HO-1 knockout mice: Pathophysiologic correlates. *Kidney Int* 68: 611–622, 2005
24. Li L, Huang L, Sung SS, Vergis AL, Rosin DL, Rose CE Jr, Lobo PI, Okusa MD: The chemokine receptors CCR2 and CX3CR1 mediate monocyte/macrophage trafficking in kidney ischemia-reperfusion injury. *Kidney Int* 74: 1526–1537, 2008
25. Kawakami T, Lichtnekert J, Thompson LJ, Karna P, Bouabe H, Hohl TM, Heinecke JW, Ziegler SF, Nelson PJ, Duffield JS: Resident renal mononuclear phagocytes comprise five discrete populations with distinct phenotypes and functions. *J Immunol* 191: 3358–3372, 2013
26. Kovtunovych G, Eckhaus MA, Ghosh MC, Ollivierre-Wilson H, Rouault TA: Dysfunction of the heme recycling system in heme oxygenase 1-deficient mice: Effects on macrophage viability and tissue iron distribution. *Blood* 116: 6054–6062, 2010
27. Kapturczak MH, Wasserfall C, Brusko T, Campbell-Thompson M, Ellis TM, Atkinson MA, Agarwal A: Heme oxygenase-1 modulates early inflammatory responses: Evidence from the heme oxygenase-1-deficient mouse. *Am J Pathol* 165: 1045–1053, 2004
28. Tzima S, Victoratos P, Kranidioti K, Alexiou M, Kollias G: Myeloid heme oxygenase-1 regulates innate immunity and autoimmunity by modulating IFN-beta production. *J Exp Med* 206: 1167–1179, 2009
29. Takahashi N, Boysen G, Li F, Li Y, Swenberg JA: Tandem mass spectrometry measurements of creatinine in mouse plasma and urine for determining glomerular filtration rate. *Kidney Int* 71: 266–271, 2007
30. Jais A, Einwallner E, Sharif O, Gossens K, Lu TT, Soyal SM, Medgyesi D, Neureiter D, Paier-Pourani J, Dalgaard K, Duvigneau JC, Lindroos-Christensen J, Zapf TC, Amann S, Saluzzo S, Jantscher F, Stiedl P, Todoric J, Martins R, Oberkofler H, Müller S, Hauser-Kronberger C, Kenner L, Casanova E, Sutterlüty-Fall H, Bilban M, Miller K, Kozlov AV, Krempler F, Knapp S, Lumeng CN, Patsch W, Wagner O, Pospisilik JA, Esterbauer H: Heme oxygenase-1 drives metaflammation and insulin resistance in mouse and man. *Cell* 158: 25–40, 2014
31. Czaikoski PG, Nascimento DC, Sônego F, de Freitas A, Turato WM, de Carvalho MA, Santos RS, de Oliveira GP, dos Santos Samary C, Tefe-Silva C, Alves-Filho JC, Ferreira SH, Rossi MA, Rocco PR, Spiller F, Cunha FQ: Heme oxygenase inhibition enhances neutrophil migration into the bronchoalveolar spaces and improves the outcome of murine pneumonia-induced sepsis. *Shock* 39: 389–396, 2013
32. Lin YT, Chen YH, Yang YH, Jao HC, Abiko Y, Yokoyama K, Hsu C: Heme oxygenase-1 suppresses the infiltration of neutrophils in rat liver during sepsis through inactivation of p38 MAPK. *Shock* 34: 615–621, 2010
33. Tracz MJ, Juncos JP, Croatt AJ, Ackerman AW, Grande JP, Knutson KL, Kane GC, Terzic A, Griffin MD, Nath KA: Deficiency of heme oxygenase-1 impairs renal hemodynamics and exaggerates systemic inflammatory responses to renal ischemia. *Kidney Int* 72: 1073–1080, 2007
34. Kotsch K, Martins PN, Klemz R, Janssen U, Gerstmayer B, Dernier A, Reutzel-Selke A, Kuckelkorn U, Tullius SG, Volk HD: Heme oxygenase-1 ameliorates ischemia/reperfusion injury by targeting dendritic cell maturation and migration. *Antioxid Redox Signal* 9: 2049–2063, 2007
35. Martins PN, Kessler H, Jurisch A, Reutzel-Selke A, Kramer J, Pascher A, Pratschke J, Neuhaus P, Volk HD, Tullius SG: Induction of heme oxygenase-1 in the donor reduces graft immunogenicity. *Transplant Proc* 37: 384–386, 2005
36. Lee TS, Chau LY: Heme oxygenase-1 mediates the anti-inflammatory effect of interleukin-10 in mice. *Nat Med* 8: 240–246, 2002
37. Soos TJ, Sims TN, Barisoni L, Lin K, Littman DR, Dustin ML, Nelson PJ: CX3CR1+ interstitial dendritic cells form a contiguous network throughout the entire kidney. *Kidney Int* 70: 591–596, 2006
38. Lee S, Huen S, Nishio H, Nishio S, Lee HK, Choi BS, Ruhrberg C, Cantley LG: Distinct macrophage phenotypes contribute to kidney injury and repair. *J Am Soc Nephrol* 22: 317–326, 2011
39. Zhang MZ, Yao B, Yang S, Jiang L, Wang S, Fan X, Yin H, Wong K, Miyazawa T, Chen J, Chang I, Singh A, Harris RC: CSF-1 signaling mediates recovery from acute kidney injury. *J Clin Invest* 122: 4519–4532, 2012
40. Poss KD, Tonegawa S: Heme oxygenase 1 is required for mammalian iron reutilization. *Proc Natl Acad Sci U S A* 94: 10919–10924, 1997
41. Zarjou A, Guo L, Sanders PW, Mannon RB, Agarwal A, George JF: A reproducible mouse model of chronic allograft nephropathy with vasculopathy. *Kidney Int* 82: 1231–1235, 2012
42. Zarjou A, Yang S, Abraham E, Agarwal A, Liu G: Identification of a microRNA signature in renal fibrosis: Role of miR-21. *Am J Physiol Renal Physiol* 301: F793–F801, 2011
43. Moon JJ, Chu HH, Hataye J, Pagán AJ, Pepper M, McLachlan JB, Zell T, Jenkins MK: Tracking epitope-specific T cells. *Nat Protoc* 4: 565–581, 2009

See related editorial, "Myeloid Cell HO-ming in AKI," on pages 2067–2069.

This article contains supplemental material online at http://jasn.asnjournals.org/lookup/suppl/doi:10.1681/ASN.2014080770/-/DCSupplemental.